

Effects of Systemic Error on Localization and Control of Differential Drive Mobile Robot

George Yuvaraj, Harisankar Suresh, Joela Jomea Shine, Abhishek Sarkar and Arshad Javed

Cite as: George, Y., Harisankar, S., Shine, J. J., Sarkar, A., & Javed, A. (2023). Effects of Systemic Error on Localization and Control of Differential Drive Mobile Robot. International Journal of Microsystems and IoT, 1(7), 437–444. <https://doi.org/10.5281/zenodo.10441392>




© 2023 The Author(s). Published by Indian Society for VLSI Education, Ranchi, India



Published online: 18 December 2023.



Submit your article to this journal: 




Article views: 



View related articles: 



View Crossmark data: 

DOI: <https://doi.org/10.5281/zenodo.10441392>



Effects of Systemic Error on Localization and Control of Differential Drive Mobile Robot

George Yuvaraj, Harisankar Suresh, Joeal Jomea Shine, Abhishek Sarkar and Arshad Javed

Department of Mechanical Engineering, Birla Institute of Technology & Science Pilani (BITS Pilani) - Hyderabad Campus, Hyderabad, Telangana 500078, India.

ABSTRACT

A novel exploration into the practical application of the Kalman filtering technique for the control and observability of a differential drive mobile robot is presented in this article. The effectiveness of Kalman filtering in addressing the localization challenges within a partially known environment is assessed. In a controlled quasi-static setting, odometric error data is meticulously collected on a metric scale, and deviations are analyzed to establish a pseudo-random error model for a differential drive robot under two scenarios: a fully functional system and a system experiencing partial failure. Surprisingly, it is found that despite calibrated odometric readings, the controller struggles to differentiate between systemic and non-systemic errors, treating both as identical. This unique challenge manifests when one or more sensors/actuators introduce non-systemic errors perceived as systemic errors. The study extends to mobile robots equipped with ultrasonic sensors, precisely delineating ranges within ± 2 cm along the heading direction, providing valuable insights into the nuanced dynamics of Kalman filtering and paving the way for future advancements in mobile robot control systems.

KEYWORDS

Autonomous Mobile Robot (AMR); Localization; Kalman Filter; Odometry; Systemic Errors Sensor Fusion;

1. INTRODUCTION

Reducing the workforce using robotic applications has been increasingly demanding in several industries. Autonomous Mobile Robots (AMRs) with capabilities to continuously perceive, process, and control a system based on the data collected concerning efficiency and continuous optimization are the driving features of industrial robots in transforming Industry 4.0 [1]. Mobile robots have a broad range of applications, not just for tracking and surveillance [2]. So, an AMR is a mechanism that carries a tool to perform diverse tasks. AMR navigation has several phases, like path planning and its feedback system, i.e., perception and control, which are essential in determining the robot's efficiency. Further, all these processes culminate in motion planning and control, where the robot's kinematics and actuators are operated to achieve the required motion and cognition. At the heart of this problem is Localization; Panigrahi et al. mention localization problems such as pose tracking (position and orientation), global localization, and kidnapped robots [3].

In the pose tracking problem, the initial position and orientation are known at the initial time 't₀'. Then the succeeding position and orientation at any time 't_n' are calculated using odometric data of the motors from the initial state. A time-bound sequential integration of odometric data for any time yields the state of the mobile robot. It is known as the dead reckoning (DR) technique [2], [3]. The global localization problem is similar to DR only when the robot does not know its initial state and relies on sensory perception and a map of the environment. This problem demands probabilistic approaches.

Finally, the kidnapped robot is a case of when it is lost, i.e., its environment becomes arbitrary. If information about the environment is available for the robot for map matching and that information is reliable, then the robot is in a known environment. For instances where there is only partial information about the robot's environment available for map matching or that information is unreliable, the robot is in a partially known environment [4].

In robotic perception, the measurement uncertainty depends on many external factors, such as thermal noise, atmospheric effects, dynamic motion, receiver clock precision, and many more, depending on the phenomenon of the sensor and its sensitivity to environmental factors. The odometric error can be probabilistic error i.e. non-systemic error and deterministic error i.e., systemic error [5], [6]. Systemic errors are not introduced by the environment but are inherited by the system in some form of inaccuracy. Typically, they are associated with the mechanical behavior of the elements in a system, such as slippage, fitting, tolerances, and non-uniform load distribution, which make one wheel turn relatively slower than the other. Non-systemic errors incur due to the robot's interaction with the environment, such as uneven terrain, temperature effects on the sensory data, and noise interference with the system.

Odometry is the simplest and the most widely used navigation method for mobile robot positioning [7]. The fundamental idea is integrating incremental motion information over time, which inevitably leads to the accumulation of errors [8]. Odometry calibration is achieved by measuring actual displacement with an anticipated displacement of the wheeled mobile robot [9]. This calibration helps to mitigate systemic errors and, if not addressed, accumulation of orientation errors will cause

significant position errors, which increase proportionally with the distance traveled by the robot [8]. Odometric calibration addresses systemic errors like the difference in the relative motion of the wheels due to asymmetric weight distribution of the wheeled mobile robot, causing one wheel to take a higher load than the other resulting in relative motion difference. Even for the robot's well-balanced center of gravity (CG), the load distribution can be uneven for terrain with a slope, resulting in relative motion differences.

From a general point of view, two standard techniques for countering the localization problem are to resolve the odometric error by sensor fusion [10] or to enhance the controllability and observability of the mobile robot [6], [11]. The sensor fusion techniques complement the error of one sensor with another in range sensing and feature detection, which eventually leads to map matching of the robot's environment [6], [12]. The second approach observes the state variables and controls or optimizes the inputs to achieve precise position and motion tracking [2]. Alternatively, made markers on the wheels to avoid the process of odometric calibrations to improve localization [13].

Antonelli et al. published a statistical-based odometric calibration technique in 2005, which presents normalized position error and orientation error of the wheeled robot [6]. The most common technique is a Kalman filter, which uses a state-space control technique and linearizes the error for small incremental motion. Appropriate state variables shall be defined for the mobile robot to deploy Kalman filtering effectively [14], [15]. If state variables are not observable, then observable parameters need to be mapped to state variables. For a mobile robot, the observable parameters are its position and velocity at any point on the trajectory. However, the controller's observable parameter is the position of the encoder, i.e., odometric reading. Odry et al. developed an adaptive Kalman filtering algorithm for low-cost gyroscopes, accelerometers, and encoders to reduce noise covariance using fuzzy logic [15]. Cheng et al. employed the dual Kalman filtering technique for stereo vision and gyroscope to reduce the covariance of individual sensing equipment to achieve higher reliability in localization [16].

Existing literature emphasizes mostly computing more precise gains, even for a dynamically varying system. The objective of this experiment is to observe the impact of systemic errors on the localization and controllability of a mobile robot.

2. METHODOLOGY

For a differential drive-wheeled mobile robot, the odometric error is observed on a metric scale for linear displacement for its state variables. The state variables essentially represent the position and orientation of the robot about its geometric center in a two-dimensional Cartesian plane (x,y) , and the robot's orientation with a global reference frame is represented by Θ . Therefore, the observable state variables are (x,y,Θ) . The differential drive-wheeled mobile robot is equipped with ultrasonic sensor HC-SR04 and DC motors with encoders. The sensor fusion of the odometric reading from the encoder and the range sensing of the ultrasonic sensor is anticipated to

complement and attenuate the AMR's systemic and non-systemic errors. Thus, it enhances the system's observability and provides a reliable feedback mechanism in the computational process. Then gain values are computed for the motor actuation to compensate for errors observed.

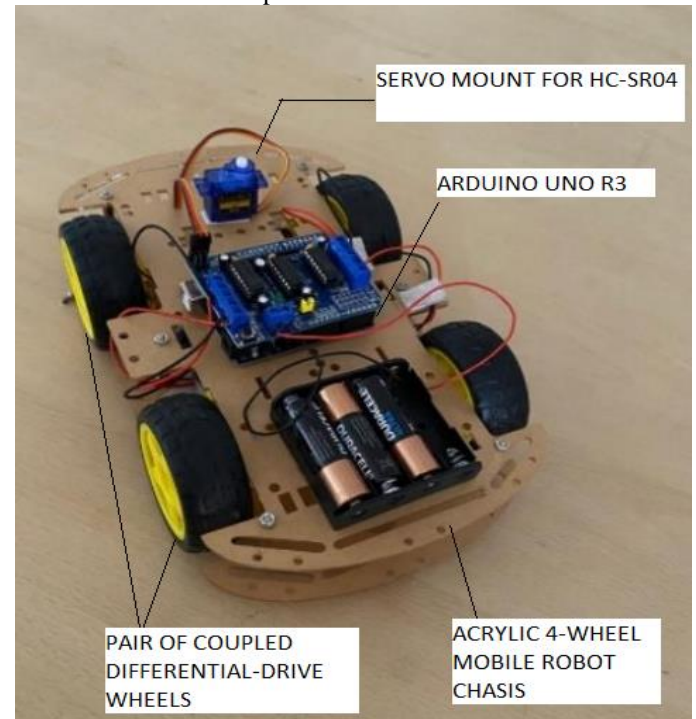


Fig. 1 Assembled differential drive robot

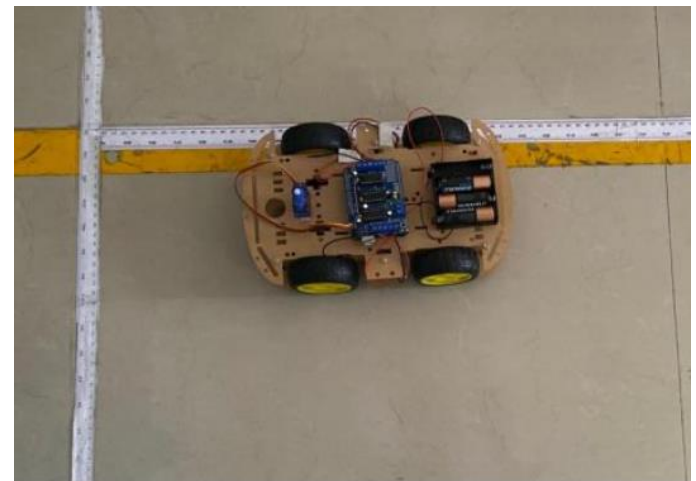


Fig. 2 Arena for odometric calibration

Table 1 AMR Specifications

MOTOR	
Voltage	5 V
Current	120 mA
RPM (no load)	280
Noise	<65 dB
Weight	50 x 4 =200 gm
Dimensions	70x22x18 mm ³
Servo Motor	Tower Pro SG 90
Wheel Diameter	66 mm
Tire width	22 mm
US SENSOR	
	HC SR04

The differential drive robot was fabricated with commercial off-the-shelf components, as shown in Fig. 1. The AMR is assembled with Quad Store 4WD (4-wheel drive) Smart Robot Car chassis of dimensions $230 \times 120 \times 5$ mm Acrylic sheets (Qty.2), Arduino UNO R3 micro-controller, Tower Pro MG90S servo motor, Duracell Ultra AA Alkaline batteries (Qty.4), L293D motor driver shield [17]. Motor specifications are tabulated in Table 1. The rear wheels of the four motors are coupled together to work as a differential drive motion robot. The arena is marked with a metric ruler scale, as seen in Fig. 2, and AMR is programmed to move at full speed (Max. PWM- Pulse Width Modulated Signal) for 0.5s with a 30s time-step to experiment with calculating errors in actuation.

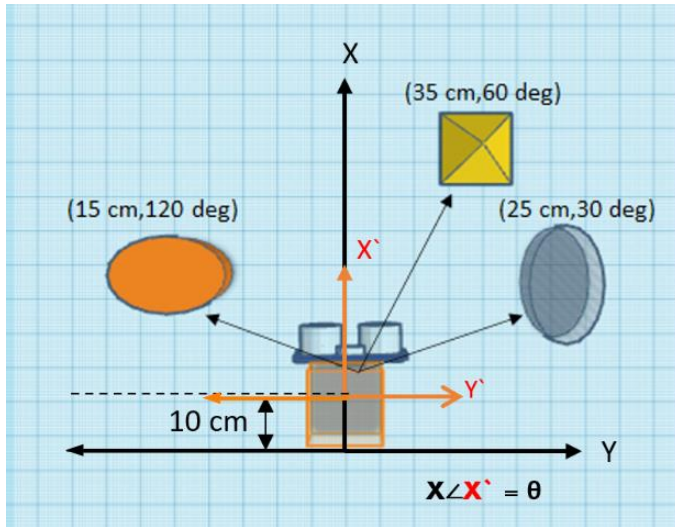


Fig. 3 Schematic diagram of experimental setup

Algorithm 1 Sensor Fusion & Kalman Filtering

Require: $P = \{[x], [y], [\theta]\}$ \triangleright Path / Map
 Initial Measure: Distance (x_n) from landmark and motor odometer \triangleright Range sensing & Odometer
 Initial Prediction: $\hat{x}_{n+1,n} = F\hat{x}_{n,n} + Gu_n + w_n$ \triangleright INITIALIZATION
 for $n > 0$ do
 Measure Odometer: $x_{n+1,n} = x_n + (2\pi r \times t \times RPM)$
 Measure Range: $x_n = C_{air}t_{echo}$ \triangleright C_{air} -sound speed
 Error: $\hat{x}_{n+1,n} - x_{n+1,n}$
 Gain: $K_n = \frac{P_n^- C^T}{C P_n^- C^T + R}$
 Update: $\hat{x}_{n,n} = \hat{x}_{n,n-1} + K_n (\alpha_n - \hat{x}_{n,n-1})$

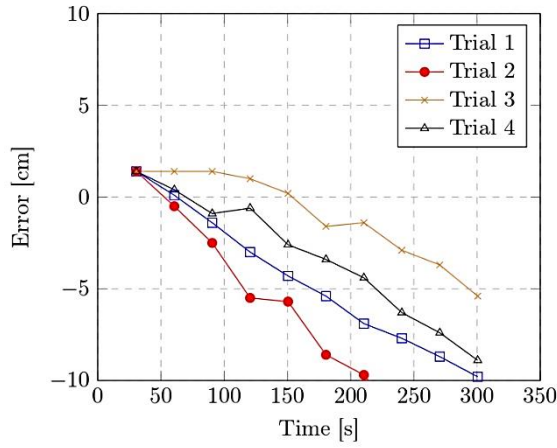
As the angular directivity range of HC SR04 is ± 25 deg, the sensor is mounted on a servo motor to increase its range and reduce the blind spot of the AMR. The servo is rotated from 10 to 175 degrees while the ultrasonic measures the distance. Three objects are placed at $35\text{cm} \times 60^\circ$, $25\text{cm} \times 30^\circ$, and $15\text{cm} \times 120^\circ$. At the same time, the radar sensor is stationary, as shown in Fig. 3. The calibrated readings are used for simulations in Python as systemic errors, and the non-system errors are introduced in the system equations as Sudo-random numbers. These simulated results are then analyzed to verify the Kalman gain estimation's effectiveness in identifying and

attenuating the errors. Algorithm 1 shows the sequence of operations for sensor fusion and the Kalman filtering technique employed in this study [18].

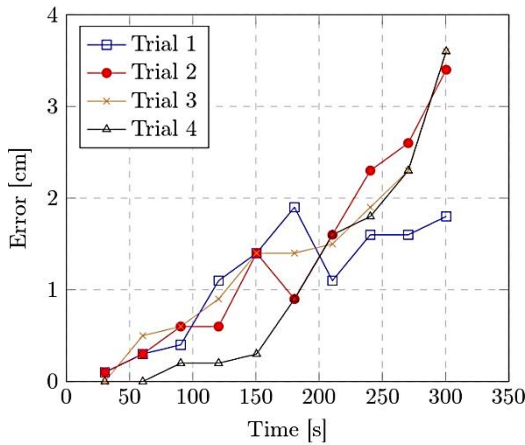
3. RESULTS AND DISCUSSIONS

Table 2 Experimental Readings

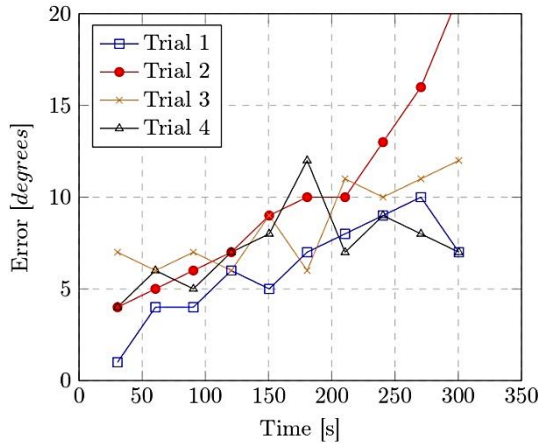
Time (s)	x (cm)	xerror (cm)	yerror (cm)	Θ_{error} (degrees)	P	K
Trial 1						
30	20	1.4	0.1	1	1.5	0.884
60	30	0.1	0.3	4	0.8	0.469
90	40	-1.4	0.4	4	0.5	0.319
120	50	-3	1.1	6	0.4	0.242
150	60	-4.3	1.4	5	0.3	0.195
180	70	-5.4	1.9	7	0.3	0.163
210	80	-6.9	1.1	8	0.2	0.140
240	90	-7.7	1.6	9	0.2	0.123
270	100	-8.7	1.6	10	0.2	0.110
300	110	-9.8	1.8	7	0.2	0.099
Trial 2						
30	20	1.4	0.1	4	1.60	0.93
60	30	-0.5	0.3	5	0.83	0.48
90	40	-2.5	0.6	6	0.56	0.33
120	50	-5.5	0.6	7	0.42	0.25
150	60	-5.7	1.4	9	0.34	0.20
180	70	-8.6	0.9	10	0.28	0.16
210	80	-9.7	1.6	10	0.24	0.14
240	90	-12.2	2.3	13	0.21	0.12
270	100	-13.7	2.6	16	0.19	0.11
300	110	-10.3	3.4	21	0.17	0.10
Trial 3						
30	20	1.4	0	7	1.30	0.76
60	30	1.4	0.5	6	0.74	0.43
90	40	1.4	0.6	7	0.52	0.30
120	50	1	0.9	6	0.40	0.23
150	60	0.2	1.4	9	0.32	0.19
180	70	-1.6	1.4	6	0.27	0.16
210	80	-1.4	1.5	11	0.23	0.14
240	90	-2.9	1.9	10	0.21	0.12
270	100	-3.7	2.3	11	0.18	0.11
300	110	-5.4	3.6	12	0.17	0.10
Trial 4						
30	20	1.4	0	4	1.48	0.86
60	30	0.4	0	6	0.80	0.46
90	40	-0.9	0.2	5	0.54	0.32
120	50	-0.6	0.2	7	0.41	0.24
150	60	-2.6	0.3	8	0.33	0.19
180	70	-3.4	0.9	12	0.28	0.16
210	80	-4.4	1.6	7	0.24	0.14
240	90	-6.3	1.8	9	0.21	0.12
270	100	-7.4	2.3	8	0.19	0.11
300	110	-8.9	3.6	7	0.17	0.10



(a) Error in X-axis



(b) Error in Y-axis

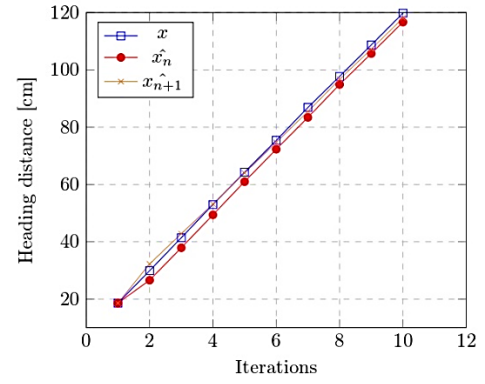


(c) Error in θ (Orientation)

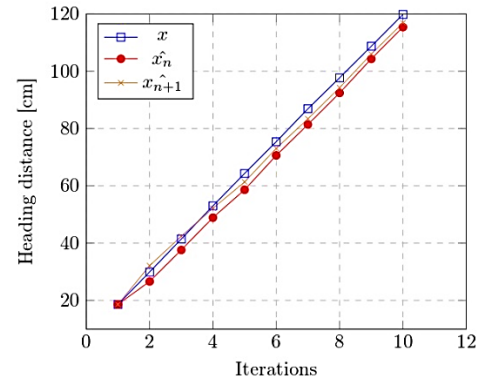
Fig. 4 Estimation of error for a translatory motion

The experiment for control error is calculated using four trials at about ten-time steps of the 30s, and sensor calibration is done using three objects at different distances and angles from each other. The experimental data are tabulated in Table 2. Table 2 contains the x, y, Θ along with Kalman gains K for four trials. Fig. 4(a), Fig. 4(b), and Fig. 4(c) show the error in the calibration with odometric data for four trials along a linear motion for three state variables, i.e., x, y , and Θ , respectively. A significant error is observed in the X-axis, i.e., in the direction of the heading, and the error in the direction of the

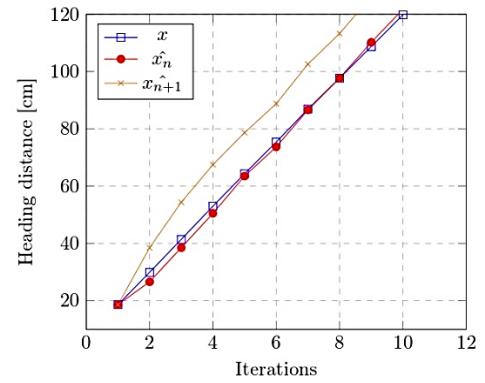
heading is twice the error in the lateral direction (Y-axis).



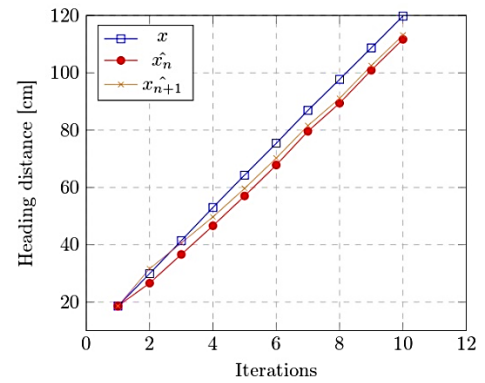
(a) Trial 1



(b) Trial 2



(c) Trial 3

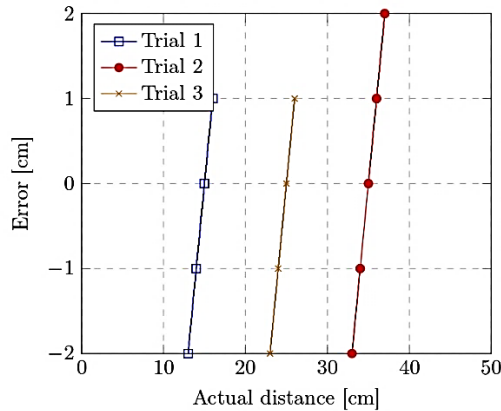


(d) Trial 4

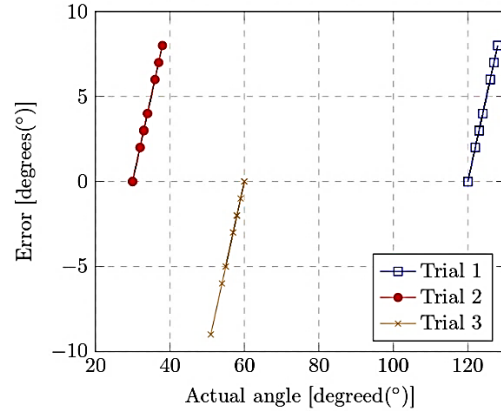
Fig. 5 Estimations for a translatory motion using Kalman filtering for odometric data

For over 6 minutes, quasi-static readings indicate the odometric error in the heading direction is nearly -10 cm, and for the Y-axis is nearly 4 cm. It is observed that the error in the direction of the heading increased steadily over time, and the other two state variables exhibited varying magnitudes of error within the range for the lateral axis (Y-axis) and orientation (Θ). Fig. 4 shows that the error in the heading direction is relatively higher, and the error in the Y-axis is negligible. The AMR employed in experiments is a differential drive-wheeled robot; it cannot have many deviations in the Y-axis without moving in the X-axis. The deviation in the lateral direction depends on the motion in the direction of the heading.

Fig. 5 shows the error of the ultrasonic sensor in identifying the landmark position and angle. From this set of experiments, it is observed that the variance of state variable Θ is 5-20 degrees, i.e., 5% maximum. The readings indicate that the error in calibrating the distance of the landmark/obstacle from a robot is between ± 2 cm.



(a) Error in position for range sensing



(b) Error in angle for range sensing

Fig. 6 Estimation of error for a translatory motion

The odometric error also induces the noisy sensor's calibration. The odometric error of the system is calibrated as 1-4 cm, and the ultrasonic sensor has an error range of ± 2 cm. Fig. 6, shows the trend of Kalman gains for four trials. The gain values converge to zero, indicating the decrease in error between estimation and the actual state. The orientation of AMR typically varies from 1-10°, but for trial two, the error was twice the error from other trials at long range. There is not much deviation of error on the lateral axis, i.e., the Y-axis, from other trials. For a differential drive mobile robot, the

orientation only changes with the relative change in motion of wheels, and orientation (Θ) cannot be independent of heading and lateral directions. Thus, the error observed in trial 2 is the sensor's, which appears as a systemic error.

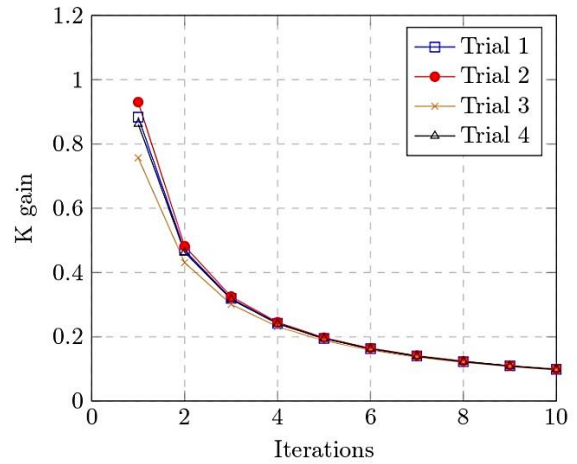


Fig. 7 Kalman gains for 4 iterations.

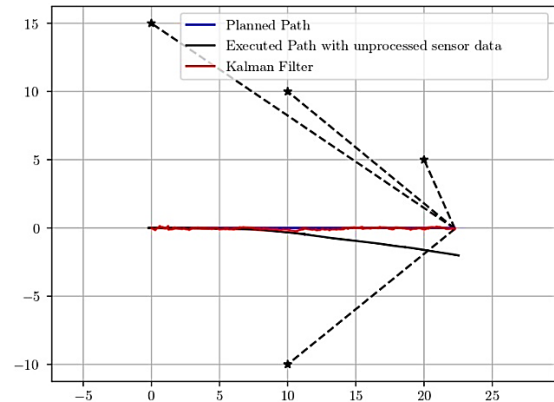


Fig. 8 Kalman filtering for a straight-line trajectory for functional case

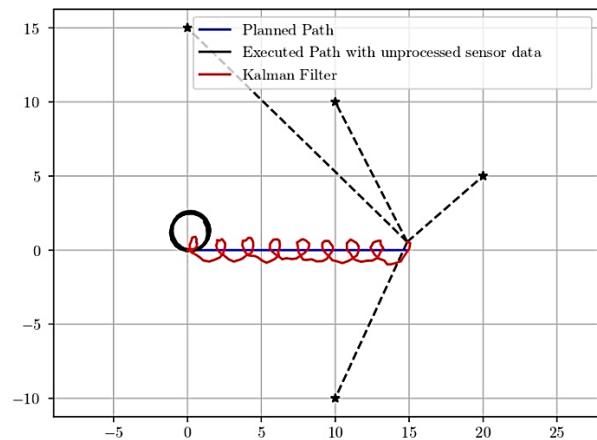


Fig. 9 Kalman filtering for a straight line trajectory with uneven actuation (partially functional case)

The observed range of deviation values is coded as an error using Sudo-random number sequences. The mobile robot is simulated in Python for various cases and the results. Thus, one-dimensional Kalman filtering is applied for four cases.

Upon subjection to Kalman filtering, the AMR behavior is shown in Fig. 7. From Fig. 7, the error in odometry is linearly proportional with each iteration. The observed range of deviation values is coded as an error using Sudo-random number sequences. The mobile robot is simulated in Python for two cases and the results. The first case is for fully functional AMR, i.e., the linear motion of the AMR while all actuators are functional, while the second is partially functional AMR when one set of motors fails. The simulation results are illustrated in Fig. 8 and Fig. 9.

This approach is linear, and the filtering technique attempts to approximate any errors induced in the execution process as linear co-efficient. The errors could be both systemic and non-systemic.

4. CONCLUSION

An experimental study of the differential drive four-wheel mobile robot was carried out using the Kalman filtering technique. What distinguishes this study is the revelation that linear gains for the system are consistently computed by Kalman filtering, even when faced with unknown kinematic and geometric constraints. Remarkably, it was demonstrated that sensor data noise is treated as systemic, showcasing the technique's resilience against increasing odometric errors over time.

Through experimentation with the HC SR04 ultrasonic sensor, a ± 2 cm error range and an angular directivity blind spot at extended distances were uncovered. Interestingly, the heading direction was identified as the primary source of significant error in mobile robots, with errors in the other two state variables proving negligible in short and medium ranges.

What truly sets this study apart is the discovery that Kalman filtering, lacking decision-making capabilities to identify system or sensor failures, computes gain values that can be physically non-realizable even for faulty components. This paradigm-shifting insight calls for a more in-depth investigation into understanding sensor noise.

The next frontier of research delves into a revolutionary approach—simultaneously incorporating decision-making capabilities and Kalman filtering. This ambitious endeavor aims to redefine the landscape by not only understanding sensor behavior but also developing a phenomenological model. This model promises higher repeatability and precision, setting the stage for a new era in mobile robot applications, according to the researchers.

REFERENCES

- [1] M. Javaid, A. Haleem, R. P. Singh, and R. Suman. (2021). Substantial capabilities of robotics in enhancing industry 4.0 implementation. *Cognitive Robotics*, 1. 58-75. <https://doi.org/10.1016/j.cogr.2021.06.001>
- [2] M. A. Mahmud, M. S. Aman, H. Jiang, A. Abdelgawad, and K. Yelamarthi. (2016). Kalman filter based indoor mobile robot navigation. in *International Conference on Electrical, Electronics, and Optimization Techniques, ICEEOT*. 1949-1953. <https://doi.org/10.1109/ICEEOT.2016.7755029>
- [3] P. K. Panigrahi and S. K. Bisoy, (2022). Localization strategies for autonomous mobile robots: A review. *Journal of King Saud University - Computer and Information Sciences*. 34 (8). 6019-6039. <https://doi.org/10.1016/j.jksuci.2021.02.015>
- [4] B. Zhang, G. Li, Q. Zheng, X. Bai, Y. Ding, and A. Khan. (2022). Path Planning for Wheeled Mobile Robot in Partially Known Uneven Terrain. *Sensors*, 22 (14). 5217. <https://doi.org/10.3390/s22145217>
- [5] K. Lee, W. Chung, and K. Yoo. (2010) Kinematic parameter calibration of a car-like mobile robot to improve odometry accuracy. *Mechatronics*, 20 (5). 582-595. <https://doi.org/10.1016/j.mechatronics.2010.06.002>
- [6] G. Antonelli, S. Chiaverini, and G. Fusco. (2005). A calibration method for odometry of mobile robots based on the least-squares technique: Theory and experimental validation. *IEEE Transactions on Robotics*. 21 (5). 994-1004. <https://doi.org/10.1109/TRO.2005.851382>
- [7] J. Borenstein. (1998). Experimental results from internal odometry error correction with the Omni Mate mobile robot. *IEEE Transactions on Robotics and Automation*. 14 (6). 963-969. <https://doi.org/10.1109/70.736779>
- [8] J. M. Armingol, A. De La Escalera, L. Moreno, and M. A. Salichs. (2002). Mobile robot localization using a non-linear evolutionary filter. *Advanced Robotics*, 16 (7). 629-652. <https://doi.org/10.1163/15685530260390755>
- [9] C. Jung and W. Chung. (2011). Calibration of kinematic parameters for two-wheel differential mobile robots by using experimental heading errors. *Int J Adv Robot Syst*. 8 (6). <https://doi.org/10.5772/50906>
- [10] P. Bikfalvi and I. Lóránt. (2000). Combining Sensor Redundancy for Fault Detection in Navigation of an Autonomous Mobile Vehicle. *IFAC Proceedings Volumes*, 33 (11). [https://doi.org/10.1016/S1474-6670\(17\)37466-9](https://doi.org/10.1016/S1474-6670(17)37466-9)
- [11] M. B. Alatise and G. P. Hancke. (2020). A Review on Challenges of Autonomous Mobile Robot and Sensor Fusion Methods. *IEEE Access*, 8. <https://ieeexplore.ieee.org/document/9007654>
- [12] Yang, M.; Sun, X.; Jia, F.; Rushworth, A.; Dong, X.; Zhang, S.; Fang, Z.; Yang, G.; Liu, B (2022). Sensors and Sensor Fusion Methodologies for Indoor Odometry: A Review. *Polymers (Basel)*, 14 (10). <https://doi.org/10.3390/polym14102019>
- [13] Y. George and A. Sarkar. (2023). A Distributed Algorithmic Approach for Simultaneous Localization and Mapping With Acoustic Sensors. in *Advances in Robotics - 6th International Conference of The Robotics Society*, New York, NY, USA: ACM, Jul. 1–6. <https://dl.acm.org/doi/10.1145/3610419.3610446>
- [14] A. Paulo Moreira, P. Costa, and J. Lima. (2020). New approach for beacons based mobile robot localization using kalman filters. in *Procedia Manufacturing*. 512-519. <https://doi.org/10.1016/j.promfg.2020.10.072>
- [15] Á. Odry, R. Fullér, I. J. Rudas, and P. Odry. (2018). Kalman filter for mobile-robot attitude estimation: Novel optimized and adaptive solutions. *Mech Syst Signal Process*, 110. 569-589. <https://doi.org/10.1016/j.ymsp.2018.03.053>
- [16] L. Cheng, B. Song, Y. Dai, H. Wu, and Y. Chen. (2017). Mobile robot indoor dual Kalman filter localisation based

on inertial measurement and stereo vision. CAAI Trans Intell Technol. 2 (4). <https://doi.org/10.1049/trit.2017.0025>

- [17] M. M. Abrar, R. Islam, and M. A. H. Shanto, (2020). An Autonomous Delivery Robot to Prevent the Spread of Coronavirus in Product Delivery System, in 2020 11th IEEE Annual Ubiquitous Computing, Electronics and Mobile Communication Conference, UEMCON 2020. 0461-0466. <https://doi.org/10.1109/UEMCON51285.2020.9298108>
- [18] N. Kumari, R. Kulkarni, M. R. Ahmed, and N. Kumar. (2021). Use of kalman filter and its variants in state estimation: A review, in Artificial Intelligence for a Sustainable Industry 4.0. 213–230. https://doi.org/10.1007/978-3-030-77070-9_13

AUTHORS



George Yuvaraj is a Research Scholar at the AI & Robotics Lab at the Department of Mechanical Engineering, BITS Pilani, Hyderabad Campus. His areas of interest are Robotics, Mathematical Modeling, and Robotic Perception. He received an M. E. (Hons) in Aircraft Engineering from the

Moscow Aviation Institute (2021), a B. Tech -Aeronautical Engineering degree from Jawaharlal Technological University Hyderabad (2017), and a Diploma in ETC from The Institution of Electronics and Telecommunication Engineers (2013), India.

Corresponding author Email: p20210046@hyderabad.bits-pilani.ac.in

Harisankar Suresh received his B.Tech degree in mechanical communication engineering from Amrita University, India, in 2021 and his M.E degree from BITS Pilani, Hyderabad Campus, India, in 2023 and currently working as Sr. Engineer R&D at lime.ai in Bengaluru, India.

Email: h20211060189@hyderabad.bits-pilani.ac.in

Joeal Jomea Shine received his B.Tech degree in mechanical communication engineering from NIT Warangal, India, in 2020 and his M.E degree from BITS Pilani, Hyderabad Campus, India, in 2023 and is currently working as a management trainee at Sona Comstar in Gurugram, India.

Email: h20211060186@hyderabad.bits-pilani.ac.in



Abhishek Sarkar is an Assistant Professor at the Department of Mechanical Engineering, BITS Pilani, Hyderabad Campus. He holds a Ph.D. in Mechanical Engineering from IIT Kanpur, an M.E. in Production Engineering from Jadavpur University, and a B.Tech. in Mechanical Engineering from Jalpaiguri Govt. Engineering College. His research interests include artificial intelligence, design and materials engineering, the design of compliant links and joints, and limb and wheeled robot navigation. He was a Senior Research Scientist in the Robotics Research Centre at IIIT Hyderabad from April 2016 to November 2020.

Email: abhisheks@hyderabad.bits-pilani.ac.in



Arshad Javed is an Associate Professor at the Department of Mechanical Engineering, BITS Pilani, Hyderabad Campus. He received a Ph.D. and M.E in Mechanical Engineering from BITS Pilani and a B.Tech. Mechanical Engineering from Bundelkhand Institute of Engineering and Technology, Jhansi, U.P. His research interests include Micro Mechanisms, Robotics and Automation systems, Mechatronic systems, and Automation of Micro-fluidic systems. He has published over 100 research papers in international journals and conferences.

Email: arshad@hyderabad.bits-pilani.ac.in